大阪大学
感染症総合教育研究拠点
CiDER
CENTER FOR
INFECTIOUS DISEASE EDUCATION
AND RESEARCH

CiDER-DP

Center for Infectious Disease Education and Research, Discussion Paper

DP016

Real-Time COVID-19 Projections in Tokyo: Lessons for Future Pandemics

Jianing Chu, The University of Tokyo

Hongtao Li, The University of Tokyo

Taisuke Nakata, The University of Tokyo

Real-Time COVID-19 Projections in Tokyo: Lessons for Future Pandemics*

Jianing Chu† Hongtao Li‡ Taisuke Nakata§

April 30, 2026

Abstract

We examine the properties of five real-time COVID-19 infection projections in Tokyo. We find that projections tended to be (i) pessimistic, (ii) less accurate during the fifth infection wave, and (iii) optimistic before the peak and pessimistic after the peak. If policymakers and the public were to utilize real-time projections in future pandemics, it would be useful for them to be aware of the properties of these projections.

JEL Codes: C53, I18, H12

Keywords: COVID-19; Pandemic; Projection.

*We thank Masakazu Emoto, Kazuya Haganuma, Naoki Maezono, and Takeshi Ojima for their detailed comments on the manuscript. We also thank Fumio Ohtake and seminar participants at the Center for Infectious Disease Education and Research at Osaka University for their insightful comments. We used large language models for language editing and readability improvements. The authors take full responsibility for the content of the manuscript. Jianing Chu is supported by JSPS Grant-in-Aid for Scientific Research (KAKENHI), Project Number 24KJ0977. Hongtao Li was supported by the Ministry of Education, Culture, Sports, Science, and Technology (MEXT), WINGS-GSDM Designing Future Society (DFS) Fellowship, Project Number 150201SP01. Taisuke Nakata is supported by JSPS Grant-in-Aid for Scientific Research (KAKENHI), Project Number 22H04927, the Center for Advanced Research in Finance at the University of Tokyo, the Research Institute of Science and Technology for Society at the Japan Science and Technology Agency, and the COVID-19 AI and Simulation Project (Cabinet Secretariat). The authors declare no conflicts of interest.

†Graduate School of Frontier Sciences, University of Tokyo, 5-1-5 Kashiwanoha, Kashiwa City, Chiba, 277-0882, Japan; Email: j-chu@g.ecc.u-tokyo.ac.jp

‡Graduate School of Public Policy, University of Tokyo, 7-3-1 Hongo, Bunkyo-ku, Tokyo, 113-0033, Japan; Email: li-hongtao@g.ecc.u-tokyo.ac.jp

§Graduate School of Economics and Graduate School of Public Policy, University of Tokyo, 7-3-1 Hongo, Bunkyo-ku, Tokyo, 113-0033, Japan; Email: taisuke.nakata@e.u-tokyo.ac.jp

1 Introduction

Real-time infection projections—projections that were released and disseminated to policymakers and the public as the event unfolded—played a key role during the COVID-19 pandemic. Policymakers used them to anticipate healthcare demand and guide decisions on lockdowns. Some projections might have affected the public's risk perceptions and their infection-prevention behaviors through their media exposure. If policymakers and the public were to utilize real-time projections again in future pandemics, it would be useful for them to be aware of the properties of these projections.

In this paper, we evaluate the properties of five real-time COVID-19 infection projections in Tokyo and analyze common patterns across these projections. We consider two projections by epidemiologists—which we will refer to as "AB 3-2" and "AB 3-3" where AB stands for the Advisory Board for COVID-19 Control of the Ministry of Health, Labour, and Welfare—and three projections by researchers from other disciplines—one by Fujii and Nakata, one by Hirata, and one by CATs (Collective Analysis Teams). The former two were regularly submitted to the government expert meeting, whereas the latter three were occasionally submitted to the government expert meeting and frequently received media attention.[1]

We use Bias(%) (Mean Percentage Error) and RMSE(%) (Root Mean Squared Percentage Error) to assess the properties of these projections. We assess the properties of projections at three levels of aggregation: the full sample (covering the entire time period), sub-samples by infection waves (fourth through eighth waves), and sub-samples by infection phases. For the phase-level analysis, we partition each wave into a rising phase—which we define as the period from the trough to two weeks before the peak—a peak phase—which we define as the four-week window centered on the peak—and a falling phase—which we define as the period from two weeks after the peak to the subsequent trough. In the Appendix, we do consider alternative definitions of these phases in the robustness analysis.

We focus on finding common patterns across these projections and abstract from comparing their accuracies. A fair comparison of projections is challenging for two reasons. First, these projections differ from each other in the timing of the projections. Projections

[1]The Japanese government assembled a team of researchers from various disciplines to conduct policy-oriented data analyses and model simulations under the project "COVID-19 AI & Simulation Project". The project began in late 2020 and continued until fall 2023 (Kitano (2025)). Fujii-Nakata and Hirata were part of this team. Other researchers involved in the project also produced projections. Although they conducted various influential analyses throughout the pandemic, we exclude their projections because their projections tended to be more in the spirit of scenario-based policy analyses than forecasting, were less frequent, and were not as long-lasting as those of Fujii-Nakata and Hirata.

would be more accurate if researchers generated projections systematically when uncertainty was low. Second, these projections might have been generated for decision makers with different objective functions. Smaller bias and RMSE are appropriate metrics for projection comparison only under certain assumptions about the objective function of the decision maker using these projections.

We highlight the following three results. First, bias tends to be positive in the full sample and in wave-by-wave sub-samples for most projections and over most forecast horizons. That is, projected infections tend to be higher than actual infections, indicating systematically pessimistic projections. Second, among the projections for which fifth-wave data are available (AB 3-3, Fujii-Nakata, and Hirata), both the absolute value of bias and RMSE tend to be substantially larger in the fifth wave (June-December 2021) than in other waves. Third, bias tends to be negative during the rising phase—indicating optimism in projections before the peak—but positive during the peak and falling phases, indicating a shift from optimism to pessimism as the infection wave intensified. In section 5, we discuss possible mechanisms behind these results.

Our work is related to the vast literature on COVID-19 projections. Within this literature, our paper is closely related to a set of papers that examine real-time COVID-19 projections. Howerton et al. (2023) examine scenario projections released by the US Scenario Modeling Hub.[2] Cramer et al. (2022) examine the ensemble forecast of the US COVID-19 Forecast Hub.[3] Manley et al. (2024) and Silk et al. (2022) examine the medium-term projections provided by Scientific Pandemic Infections Group on Modelling (SPI-M/SPI-M-O) of Scientific Advisory Group for Emergencies (SAGE).[4] Keeling et al. (2022) examine the six roadmap projections provided by the SPI-M-O of SAGE. Sherratt et al. (2023) examined the multi-model ensemble forecast provided by the European COVID-19 Forecast

[2]The US COVID-19 Scenario Modeling Hub (SMH), created in December 2020, convened multiple modeling teams to produce months-ahead, scenario-based probabilistic projections of COVID-19 burden in the United States, from February 2021 to November 2022. See https://covid19scenariomodelinghub.org/.

[3]The COVID-19 Forecast Hub, founded in March 2020, served as a centralized repository for forecasts submitted by more than 50 international research teams. In each week, the Hub aggregated the submitted models into an ensemble forecast and made both the ensemble and individual forecasts accessible through an interactive visualization dashboard. All forecasts are also shared with the US CDC (Centers for Disease Control and Prevention), and both team-level predictions and the ensemble are incorporated into official CDC communications about the COVID-19 trajectory from April 2020 to February 2023. See https://covid19forecasthub.org/doc/.

[4]SPI-M is an expert advisory group to the UK Department of Health and Social Care that provides scientific input on the UK response to pandemics and other emerging infectious-disease threats, drawing on infectious-disease modeling, epidemiology, and related analyses. During COVID-19, it operated as SPI-M-O, an operational subgroup of SAGE that synthesized modelling evidence for government decision-making. It provided medium-term projections on a near-weekly basis and released roadmap projections in discrete rounds aligned with reopening decisions. See https://assets.publishing.service.gov.uk/media/69665f021f94f51fd079cbab/spi-m-terms-of-reference-january-2026.pdf.

Hub. Doornik et al. (2022) examine their independent real-time, short-term forecasts for the UK and EU and the forecasts.[5] We contribute to this literature by providing novel evidence on the performance of real-time COVID-19 projections using previously unexplored data from Japan.

To the best of our knowledge, ex-post evaluations of real-time projections are scarce in Japan. Among the few are Beppu et al. (2025), Nakata and Okamoto (2025), and Nakata et al. (2025). Beppu et al. (2025) examine the accuracy of the average of a few real-time projections in Tokyo—including Hirata and CATs projections in a few infection waves (sixth and seventh waves)—and find that the average tends to be more accurate than each projection. We differ from Beppu et al. (2025) because we analyze common patterns across multiple projection models over multiple waves, instead of focusing on the performance of model averaging. Nakata and Okamoto (2025) evaluate the real-time projections of severity and case fatality rates in the sixth wave. Nakata et al. (2025) conduct ex-post evaluations of a model-based real-time analysis on the likely effect of the Tokyo Olympic and Paralympic Games on infection outcomes. Fujii and Nakata (2021), Rashed and Hirata (2021a), Rashed and Hirata (2021b), and Rashed et al. (2022) examine projection accuracies of variants of the models they used for real-time projections *using past data* to demonstrate the validity of their models, but do not evaluate their real-time projections.[6]

The rest of the paper is structured as follows. Section 2 describes the data. Section 3 presents the methodology. Section 4 presents the results. Section 5 discusses possible mechanisms for our main takeaways. Section 6 concludes.

2 Data

In this section, we describe five real-time COVID-19 projections we consider in this paper.

2.1 AB 3-2

The National Institute of Infectious Diseases (NIID) regularly submitted a report containing various data and analyses to the Advisory Board for COVID-19 Control of the

[5] See also Li et al. (2023) that examine real-time projections in more than 200 geographical areas and Bosse et al. (2022) that examine real-time projections in Germany and Poland.

[6] Some researchers occasionally provided informal assessments of their real-time projections as they released their new projections, but they are infrequent, are only available in the form of presentation slides, and are only available in the Japanese language. See, for example, Kawawaki and Nakata (2023) and Beppu et al. (2021).

Ministry of Health, Labour and Welfare" throughout the COVID-19 pandemic. The Advisory Board was convened for the first time on February 7, 2020 and for the last time on August 4, 2023. They met almost every week in 2021 and 2022. From January 12, 2022 to April 17, 2023, the report by the NIID—often numbered "3-2"—included an infection projection for Tokyo, which we will refer to as the "AB 3-2" projection.[7] [8]

AB 3-2 projection is based on a statistical model of the effective reproductive number implemented in the R package EpiNow2. The projected effective reproductive number is converted to projections of new infections in the report. The model is specified at a daily frequency, and the projection horizon is seven days. There are 53 AB 3-2 projections during the aforementioned period, covering the sixth through eighth infection waves.

Each AB 3-2 report includes a table reporting projected infections. We manually extract the projected infection values from this table from each AB 3-2 report. We convert the projection from daily new infections to a 7-day moving average of new daily infections for comparability with other projections. Figure 1 shows the infection projection of AB 3-2—shown by red dots, together with the actual infection—shown by the solid black line.

2.2 AB 3-3

Hiroshi Nishiura of Kyoto University regularly submitted a report containing various analyses to the Advisory Board throughout the COVID-19 pandemic.[9] His report—often numbered "3-3"—contained a wide range of influential analyses from real-time estimates of the effective reproductive number and scenario-based analyses of lockdowns to the estimates of susceptible population and the outlook for vaccine rollout. From April 6, 2021, to November 21, 2022, the AB 3-3 report contained infection projection based on time-series models, which we refer to as the "AB 3-3" projection.

AB 3-3 reports during the aforementioned period showed infection projections from four time-series models of the effective reproductive number: (i) a constant, (ii) linear trend extrapolation, (iii) autoregression, and (iv) the simple ensemble of the first three models. The first "constant" model assumes that the effective reproduction number stays constant at the last observed estimate over the projection horizon. We focus on the simple ensemble projection in our analysis. The model is specified at a daily frequency. There are 79 reports from April 6, 2021, to November 21, 2022, covering the fourth through the early

[7] The AB is on a near-weekly basis during January 2022-January 2023, while shifting to a two-week interval during January-April 2023.

[8] See https://www.mhlw.go.jp/stf/seisakunitsuite/bunya/0000121431_00333.html.

[9] See https://www.mhlw.go.jp/stf/seisakunitsuite/bunya/0000121431_00216.html.

eighth waves.[10] The first 11 reports—covering the fourth wave and the initial part of the fifth wave—featured a 13-day projection horizon, while subsequent reports extended the horizon to 38 days.

We use a digitization tool—WebPlotDigitizer—to digitize projection data in each AB 3-3 file.[11] In some files, the projection trajectory exceeds the vertical scale of the source graph, rendering the values unobservable. To address this data truncation problem, we fit an exponential function to the visible segment of the projection to extrapolate and estimate the values that lie beyond the graph's limits. Similar to AB 3-2, we adjust the actual and projected data in AB 3-3 files to a 7-day moving average format. Figure 2 shows the infection projections of AB 3-3 over a four-week horizon—shown by dashed red lines, together with the actual infection—shown by the solid black line.

2.3 Fujii-Nakata

Daisuke Fujii and Taisuke Nakata, researchers at the University of Tokyo, regularly released COVID-19 infection projections over the 2021-2023 period. They presented their projections as well as a wide range of real-time policy analyses to policymakers and their scientific advisers on numerous occasions.[12] Fujii and Nakata produced scenario-based projections using a macro-SIR model as described in Fujii and Nakata (2021) and Haganuma et al. (2025). Their model is specified at a weekly frequency. They provided a 7-day moving average of new infection projections with horizons ranging from 10 to 54 weeks. There are 70 reports from January 2021 to March 2023, covering the fourth through eighth waves.[13] We obtain their projections from their original data files. Figure 3 shows the infection projections of Fujii-Nakata with a horizon of four weeks—shown by dashed red lines, together with the actual infection—shown by the solid black line.

[10]The projections in AB 3-3 were submitted to the AB on a near-weekly basis during April 2021-November 2022.

[11]See https://automeris.io/.

[12]See a book written by Daisuke Fujii and Taisuke Nakata, Nakata and Fujii (2022) (https://www.u-tokyo.ac.jp/biblioplaza/en/J_00092.html).

[13]Fujii and Nakata released projections on a near-weekly basis during peak periods (January-September 2021 and January-March 2022), while shifting to a two-week interval during interim periods (October 2021-January 2022, April-October 2022, and December 2022-March 2023). See, for example, https://covid19outputjapan.github.io/JP/index.html and https://www.bicea.e.u-tokyo.ac.jp/. Fujii-Nakata projections were often cited by media. See Asahi (2021), Mainichi (2022) , and Nikkei (2021b), among many others.

2.4 Hirata

Professor Akimasa Hirata of Nagoya Institute of Technology regularly submitted COVID-19 infection projections to the COVID-19 AI and Simulation Project, a project assembled by the Cabinet Office of the Japanese Government.[14] Hirata's projection is based on a deep-learning model described in Rashed and Hirata (2021a), Rashed and Hirata (2021b), and Rashed et al. (2022), which takes into account various factors such as temperature, humidity, and public mobility. The model is specified at a daily frequency. They provided 7-day moving averages of new infection projections with horizons ranging from 15 to 203 days. There are 16 reports from August 8, 2021, to April 25, 2023, covering the fifth through eighth infection waves.[15] We digitize Hirata's projections from his reports. Figure 4 shows the infection projections of Hirata with a horizon of four weeks—shown by dashed red lines, together with the actual infection—shown by the solid black line.

2.5 CATs

CATs ("Collective Analysis Teams")—a team of data scientists led by Yamaneko Research Institute, Inc.—regularly published their projections from January 24, 2022, to January 19, 2023.[16] CATs' projection is based on a machine-learning model, which incorporates factors such as traffic volume, SNS, and internet search. The model is specified at a daily frequency. They provided 7-day moving averages of new infection projections with horizons ranging from 5 to 51 days. They released 72 reports from January 24, 2022, to January 19, 2023, covering the sixth through eighth infection waves.[17]

We digitize CATs' projections from their reports published on then-Twitter (now X).[18] Figure 5 shows the infection projections of CATs over a four-week horizon—shown by dashed red lines, together with the actual infection—shown by the solid black line.

[14] See https://www.caicm.go.jp/action/survey/covid19-ai.jp/en-us/researcher/akimasa-hirata/index.html. Hirata projections were often cited by media. See, for example, Yomiuri (2022), Chunichi (2020), and Nikkei (2021a), among many others.

[15] Hirata released projections on a near-weekly basis during August-September 2021, January-February 2022, and July 2022.

[16] See https://yamaneko.co.jp/news/2022-01-25/ and Nikkei (2022c).

[17] CATs released projections nearly every weekday during two periods (January-March 2022 and July-September 2022) before shifting to a weekly schedule (December 2022-January 2023). CATs projections were often cited by media. See, for example, Nikkei (2022b) and Nikkei (2022a), among many others.

[18] CATs published their projection reports on a website—Quick Money World (https://moneyworld.jp/)—run by Quick, a financial information services company, as well as on Twitter (now X) of Lully Miura, the president of Yamaneko Research Institute, Inc. See https://x.com/lullymiura?s=21&t=jXHNe6iBitz6X0-2Fqqf4w.

3 Methodology

We use two metrics to analyze the properties of the five projection models discussed in the previous section: Bias(%) (Mean Percentage Error) and RMSE(%) (Root Mean Squared Percentage Error). All projection models except Fujii-Nakata are specified at a daily frequency. For these daily-frequency projections, we focus on a 7-day moving average of daily new infections for 7-day, 14-day, and 28-day horizons. For simplicity, we call these horizons one-week, two-week, and four-week ahead.

For each projection model, m, and for each projection horizon, h, $\text{Bias}_m^h(\%)$ is given by

$$\text{Bias}_m^h(\%) = \frac{1}{T_m^h} \sum_{t=1}^{T_m^h} \frac{\hat{y}_{m,t+h} - y_{m,t+h}}{y_{m,t+h}} \times 100. \tag{1}$$

where T_m^h denotes the number of samples for the model m with horizon of h week(s). The terms $\hat{y}_{m,t+h}$ and $y_{m,t+h}$ denote the projected and actual new infection for the projection issued at t with horizon h week(s), respectively. The term $\frac{\hat{y}_{m,t+h} - y_{m,t+h}}{y_{m,t+h}} \times 100$ is the percentage error.

For each projection model m, and for each projection horizon $h \in \{1, 2, 4\}$, $\text{RMSE}_m^h(\%)$ is given by

$$\text{RMSE}_m^h(\%) = \sqrt{\frac{1}{T_m^h} \sum_{t=1}^{T_m^h} \left(\frac{\hat{y}_{m,t+h} - y_{m,t+h}}{y_{m,t+h}} \times 100 \right)^2}, \tag{2}$$

We use Bias(%) and RMSE(%) instead of Bias (Mean Error) and RMSE (Root Mean Squared Error) because the peak infection numbers varied significantly across different waves. Using Bias and RMSE would penalize the projection during high-infection phases and makes cross-wave comparisons invalid.

We compute these two metrics—Bias(%) and RMSE(%)—for each projection and for each forecast horizon using the entire sample. We also compute these metrics for each projection and for each forecast horizon in sub-samples grouped by infection waves and by infection phases—rising, peak, and falling phases. To define infection phases, we first identify the trough—the lowest infection point—and the peak for each infection wave based on actual infection data.[19] We then define three infection phases—rising, peak, and falling—as follows: The rising phase extends from the trough to two weeks before the peak; the peak phase covers the interval from two weeks before to two weeks after the peak; and the falling phase runs from two weeks after the peak to the subsequent

[19] We identify peak and trough dates at a daily frequency for all models except Fujii-Nakata, where we identify them at a weekly frequency.

trough. In addition to this baseline definition of these three phases, we will also consider alternative phase definitions. Our main takeaways are robust to alternative definitions.

We also compute overall Bias(%) and overall RMSE(%) including all available projections—as opposed to projection-by-projection—for the entire sample, wave-by-wave and phase-by-phase subsamples. These metrics would summarize the common patterns across projections concisely. Specifically, for each projection horizon, $\text{Bias}^h(\%)$ is given by

$$\text{Bias}^h(\%) = \frac{1}{\sum_{m=1}^{5} T_m^h} \sum_{m=1}^{5} \sum_{t=1}^{T_m^h} \frac{\hat{y}_{m,t+h} - y_{m,t+h}}{y_{m,t+h}} \times 100, \tag{3}$$

and $\text{RMSE}^h(\%)$ is given by

$$\text{RMSE}^h(\%) = \sqrt{\frac{1}{\sum_{m=1}^{5} T_m^h} \sum_{m=1}^{5} \sum_{t=1}^{T_m^h} \left(\frac{\hat{y}_{m,t+h} - y_{m,t+h}}{y_{m,t+h}} \times 100 \right)^2}. \tag{4}$$

where $m = \{1, 2, 3, 4, 5\}$ is an index for each of the five real-time projections.

As discussed in the introduction, we focus on characterizing common patterns across five real-time projections, without comparing accuracy across projections. There are two reasons for this focus. First, there are differences in the timing of projection releases among projections. For example, Hirata and CATs typically began releasing their projections when the infection wave intensified and was approaching the peak, and ceased publication once a clear decline became evident. In contrast, AB 3-2, AB 3-3, and Fujii-Nakata released projections more regularly through different phases of infection waves, including when infections were near the trough. If it were easier or more difficult to project infection in some periods than in other periods, and some release their projections systematically when projections are easier or more difficult, we would risk misjudging the model's projection accuracy.

Second, a fair evaluation of a projection requires the objective function of the decision maker using that projection. If policymakers are robust policymakers wishing to avoid the worst-case scenario, the optimal projection may feature positive bias. Because the five projections were prepared for different audiences for different reasons, simple comparisons of Bias(%) and RMSE(%) across projections are unlikely to be informative.

4 Results

4.1 Baseline Results

Table 1 shows RMSE(%) and bias(%) for the entire sample. According to the table, the magnitude of Bias(%) and RMSE(%) rise with the projection horizon for each projection and for all projections combined, indicating that projections are less accurate for a longer horizon than for a shorter horizon. Bias(%) is positive across most projections and horizons with only a few exceptions, indicating that these real-time projections tend to be pessimistic. Bias(%) for all projections is also positive for all three projection horizons.

Table 2 presents the results of wave-by-wave subsample analysis. According to these tables, bias(%) tends to be positive for most projections and for most projection horizons. Bias(%) is positive over all three horizons for the fifth to eighth waves for Fujii-Nakata, for the fifth, sixth, and eighth waves for Hirata, and for the seventh and eighth waves for CATs. For AB 3-2 and AB 3-3 projections, however, we observe negative biases just as often as positive biases. When all projections are combined, we observe that bias(%) is positive for most waves and for most projections.

Another takeaway from the wave-by-wave analysis is that the fifth wave was the most challenging projection period. Across AB 3-3, Fujii-Nakata, and Hirata (the models available for the fifth wave), RMSE(%) is notably larger in the fifth wave than in other waves, with one-week ahead projections by Fujii-Nakata being only one exception. We observe the difficulty of projection in the fifth wave in the magnitude of Bias(%) as well. When all projections are combined, RMSE(%) is still the largest in the fifth wave among all waves.

Table 3 shows RMSE(%) and bias(%) for rising, peak, and falling phases. According to the table, Bias(%) tends to be negative during the rising phase but positive during the peak and falling phases. Bias(%) is negative during the rising phase across all horizons of all projections, except for the one-week ahead projection of Fujii-Nakata. Bias(%) is positive during the peak phase for all projections over all projection horizons. Bias(%) remains positive during the falling phase for all projection horizons of all projections, except for the one- and two-week ahead projections of AB 3-3 and the one-week ahead projection of Hirata. When all projections are combined, the pattern is even clearer. Bias(%) is negative during the rising phase and positive during the peak and falling phases for all three horizons. This result regarding phase-dependent bias(%) are qualitatively robust to alternative definitions of phases. See Appendix A in which we conduct phase-by-phase analysis under two alternative definitions of phases.

In addition, for projections with longer horizons (two and four weeks), RMSE(%) tends to be larger during the peak and falling phases than during the rising phase, imply-

ing a lower reliability of long-term projections during the peak and falling phases. This phase-dependence in RMSE(%) is less apparent for one-week-ahead projections, but is evident for two- and four-week-ahead projections.

5 Discussion

The first result regarding the overall bias may hold because policymakers might have welcomed pessimistic projections more than optimistic projections. Underreacting to a fast-growing outbreak might have been perceived as far more costly than overreacting. If policymakers treat false negatives as more dangerous than false positives, they may prefer pessimistic projections as a safer decision guide. Policymakers might have welcomed pessimistic projections also because pessimistic projections help with public compliance.

The second result regarding larger RMSE and bias in the fifth wave may hold because a number of factors introduced uncertainty in the infection outlook as the fifth wave unfolded. Those factors include, but are not limited to, the spread of the Delta variant, the hosting of the Tokyo Olympic Games, and the start of the large-scale vaccine rollout around June 2021. These factors created uncertainty, which might have raised the difficulty of infection projections during this period.

The third result regarding the shift in bias over the infection cycle may arise if projections respond to the development in infection outcomes with a lag. In the early phase of an infection wave, projections are still informed by recent data on low and stable infection. As actual infection rises further, the public becomes more alert and acts more cautiously, which decelerates the rise in infection and eventually puts an end to the infection wave. However, projections tend to react to the deceleration in actual infection with a lag and continue to project further increases in infection, making them more pessimistic.

6 Conclusion

In this paper, we investigated common patterns across five real-time COVID-19 infection projections in Tokyo. We obtained the following three takeaways. First, bias tends to be positive in the full sample and in wave-by-wave sub-samples for most projections and over most forecast horizons. That is, projected infections tend to be higher than actual infections, indicating systematically pessimistic projections. Second, among the projections for which fifth-wave data are available (AB 3-3, Fujii-Nakata, and Hirata), both the absolute value of bias and RMSE tend to be larger in the fifth wave (June-December 2021)

than in other infection waves. Third, bias tends to be negative during the rising phase—indicating optimism in projections before the peak—but positive during the peak and falling phases, indicating a shift from optimism to pessimism as the infection wave intensified.

Infection projections played a key role in informing policymakers and the public during the COVID-19 pandemic. They are likely to play a key role in future pandemics as well. Even though a number of infection projections were produced and disseminated to policymakers and the public during the COVID-19 pandemic in Japan, ex-post evaluations of these real-time projections are scarce. Our research fills only a part of the large gap in the knowledge. Further evaluations are likely to be valuable in helping us better prepare for future pandemics.

References

Asahi, S. (2021). With another emergency declaration possible after restrictions are lifted, researchers stress the importance of risk management. *The Asahi Shimbun*. https://www.asahi.com/articles/ASP3473HHP34ULBJ00R.html.

Beppu, S., D. Fujii, S. Kawawaki, Y. Maeda, and T. Nakata (2021). Discrepancies between the baseline scenario and the actual outcome. Mimeo, University of Tokyo. https://covid19outputjapan.github.io/JP/files/FujiiNakata_ProjectionReview_20211214.pdf.

Beppu, S., S. Miyashita, and T. Nakata (2025). Forecasting COVID-19 Infection with Model Averaging: A Real-Time Evaluation. In S. Kurihara (Ed.), *Social Simulation of COVID-19 with AI in Japan: Multi-agent Simulation, Multi-layered AI Simulation, Deep Learning-Based Modelling, and Beyond*, pp. 181–190. Singapore: Springer Nature.

Bosse, N. I., S. Abbott, J. Bracher, H. Hain, B. J. Quilty, M. Jit, Centre for the Mathematical Modelling of Infectious Diseases COVID-19 Working Group, E. van Leeuwen, A. Cori, and S. Funk (2022). Comparing human and model-based forecasts of COVID-19 in Germany and Poland. *PLOS Computational Biology 18*(9), e1010405.

Chunichi, S. (2020). AI forecast by Nagoya Institute of Technology: January infections could fall 60% if mobility in Aichi drops 20%. *Chunichi Shimbun*. https://www.chunichi.co.jp/article/168959.

Cramer, E. Y., E. L. Ray, V. K. Lopez, J. Bracher, A. Brennen, A. J. Castro Rivadeneira, A. Gerding, T. Gneiting, K. H. House, Y. Huang, et al. (2022). Evaluation of individual and ensemble probabilistic forecasts of COVID-19 mortality in the United States. *Proceedings of the National Academy of Sciences of the United States of America 119*(15), e2113561119.

Doornik, J. A., J. L. Castle, and D. F. Hendry (2022). Short-term forecasting of the coronavirus pandemic. *International Journal of Forecasting 38*(2), 453–466.

Fujii, D. and T. Nakata (2021). COVID-19 and output in Japan. *The Japanese Economic Review 72*(4), 609–650.

Haganuma, K., T. Nakata, and W. Okamoto (2025). Prefecture-Level Projections for COVID-19 Hospital Bed Demand in Japan. In S. Kurihara (Ed.), *Social Simulation of COVID-19 with AI in Japan: Multi-agent Simulation, Multi-layered AI Simulation, Deep Learning-Based Modelling, and Beyond*, pp. 53–62. Singapore: Springer Nature.

Howerton, E., L. Contamin, L. C. Mullany, M. Qin, N. G. Reich, S. Bents, R. K. Borchering, S.-m. Jung, S. L. Loo, C. P. Smith, et al. (2023). Evaluation of the US COVID-19 Scenario Modeling Hub for informing pandemic response under uncertainty. *Nature Communications 14*(1), 7260.

Kawawaki, S. and T. Nakata (2023). Discrepancies between the baseline scenario and the actual outcome: 2022. Mimeo, University of Tokyo. https://www.bicea.e.u-tokyo.ac.jp/wp-content/uploads/2023/01/7039db1e663a7a7a7578902d100336b3.pdf.

Keeling, M. J., L. Dyson, M. J. Tildesley, E. M. Hill, and S. Moore (2022). Comparison of the 2021 COVID-19 roadmap projections against public health data in England. *Nature Communications 13*(1), 4924.

Kitano, H. (2025). Mission-critical policy decisions in a pandemic: Japan's use of AI and complex systems simulation in COVID-19 response. In S. Kurihara (Ed.), *Social Simulation of COVID-19 with AI in Japan: Multi-agent Simulation, Multi-layered AI Simulation, Deep Learning-Based Modelling, and Beyond*, pp. 1–17. Singapore: Springer Singapore.

Li, M. L., H. T. Bouardi, O. S. Lami, T. A. Trikalinos, N. Trichakis, and D. Bertsimas (2023). Forecasting COVID-19 and Analyzing the Effect of Government Interventions. *Operations Research 71*(1), 184–201.

Mainichi, S. (2022). UTokyo team predicts: COVID cases in Tokyo in May exceeds 10,000 per day; peak seen in first week of next month. *The Mainichi Shimbun*. https://mainichi.jp/articles/20220119/ddm/002/040/102000c.

Manley, H., T. Bayley, G. Danelian, L. Burton, T. Finnie, A. Charlett, N. A. Watkins, P. Birrell, D. De Angelis, M. Keeling, S. Funk, G. Medley, L. Pellis, M. Baguelin, G. J. Ackland, J. Hutchinson, S. Riley, and J. Panovska-Griffiths (2024). Combining models to generate consensus medium-term projections of hospital admissions, occupancy and deaths relating to COVID-19 in England. *Royal Society Open Science 11*(5), 231832.

Nakata, T., A. Chiba, D. Fujii, Y. Maeda, M. Mori, K. Nagasawa, and W. Okamoto (2025). The effects of hosting the Olympic and Paralympic Games on COVID-19 in Tokyo: Real-time analyses and ex-post evaluation. *The Japanese Economic Review*.

Nakata, T. and D. Fujii (2022). *COVID-19 Crisis: A Tale of Two Economists*. Tokyo: Nippon Hyoron Sha. https://www.u-tokyo.ac.jp/biblioplaza/en/J_00092.html.

Nakata, T. and W. Okamoto (2025). Projections of COVID-19 severity and case fatality rates in Tokyo: Real-time analysis and ex-post assessment. In S. Kurihara (Ed.), *Social Simulation of COVID-19 with AI in Japan: Multi-agent Simulation, Multi-layered AI Simulation, Deep Learning-Based Modelling, and Beyond*, pp. 41–52. Singapore: Springer Nature.

Nikkei, S. (2021a). Nagoya Institute of Technology forecast by Prof. Hirata: Sixth-wave daily COVID cases could be around 200 in mid-January. *Nikkei*. https://www.nikkei.com/article/DGXZQOFD224S40S1A121C2000000/.

Nikkei, S. (2021b). Prime Minister cautions about risk of another state of emergency as hospital beds remain under strain. *Nikkei*. https://www.nikkei.com/article/DGXZQODE111SY0R10C21A2000000/.

Nikkei, S. (2022a). Tokyo's COVID infections seen peaking in early January in private forecast. *Nikkei*. https://www.nikkei.com/article/DGXZQOCC277TD0X21C22A2000000/.

Nikkei, S. (2022b). Tokyo's seventh-wave COVID cases seen near 50,000 in early August in private forecast. *Nikkei*. https://www.nikkei.com/article/DGXZQOCC275HE0X20C22A7000000/.

Nikkei, S. (2022c). Turning Big Data into a tool for the Prime Minister's Office: Tatsu Fukuda and others' search for a way forward. *Nikkei*. https://www.nikkei.com/article/DGXZQOCD258NK0V20C22A2000000/.

Rashed, E. A. and A. Hirata (2021a). Infectivity Upsurge by COVID-19 Viral Variants in Japan: Evidence from Deep Learning Modeling. *International Journal of Environmental Research and Public Health 18*(15), 7799.

Rashed, E. A. and A. Hirata (2021b). One-Year Lesson: Machine Learning Prediction of COVID-19 Positive Cases with Meteorological Data and Mobility Estimate in Japan. *International Journal of Environmental Research and Public Health 18*(11), 5736.

Rashed, E. A., S. Kodera, and A. Hirata (2022). COVID-19 forecasting using new viral variants and vaccination effectiveness models. *Computers in Biology and Medicine 149*, 105986.

Sherratt, K., H. Gruson, R. Grah, H. Johnson, R. Niehus, B. Prasse, F. Sandmann, J. Deuschel, D. Wolffram, S. Abbott, et al. (2023). Predictive performance of multi-model ensemble forecasts of COVID-19 across European nations. *eLife 12*, e81916.

Silk, D. S., V. E. Bowman, D. Semochkina, U. Dalrymple, and D. C. Woods (2022). Uncertainty quantification for epidemiological forecasts of COVID-19 through combinations of model predictions. *Statistical Methods in Medical Research 31*(9), 1778–1789.

Yomiuri, S. (2022). Tokyo COVID cases seen at 6,000 in late March; could reach nearly 14,000 by mid-April if mobility increases. *Yomiuri Shimbun*. https://www.yomiuri.co.jp/medical/20220320-OYT1T50198/.

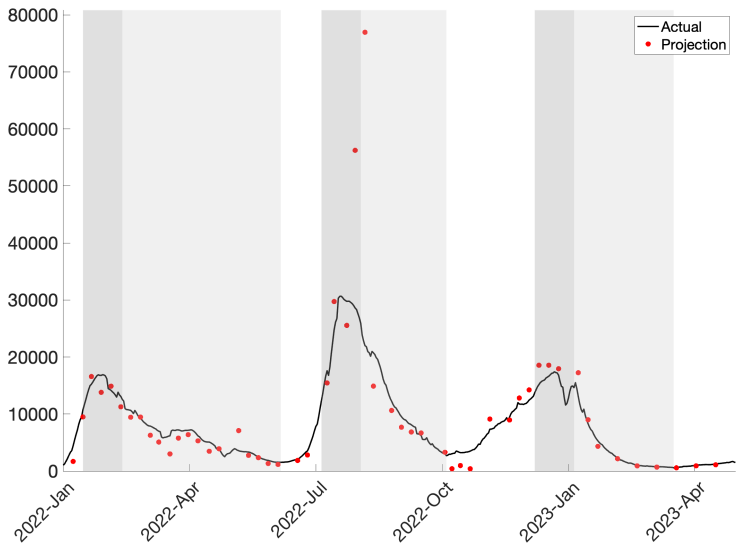

Figure 1: AB 3-2 Projection

Note: The red dots show one-week-ahead projections of the 7-day moving average of daily new infections. Projection data are from the numerical tables in the original reports. The solid black line shows the actual 7-day moving average of daily new infections at a daily frequency. In AB 3-2 projection, the actual data is from HER-SYS. However, access to HER-SYS is restricted, we collect the actual infection data by digitizing each AB 3-2 file using a digitization tool (WebPlotDigitizer). The actual infection data ends on April 14, 2023 in the last AB 3-2 report. The subsequent actual data is from the Tokyo Metropolitan Government.

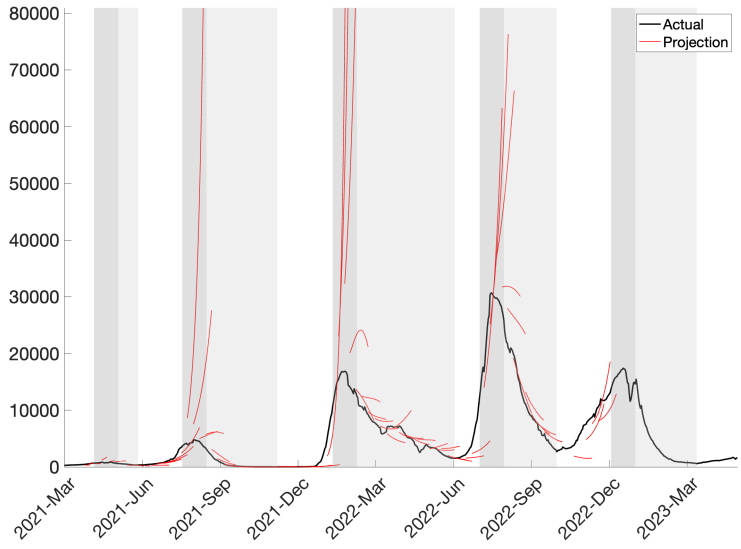

Figure 2: AB 3-3 Projection

Note: The solid red lines show projections of the 7-day moving average of daily new infections at a daily frequency over the four-week projection horizon. Projection data are digitized from the original reports. We employ an exponential fitting model to extrapolate the projection when its trajectory exceeds the vertical scale of the source graph. The solid black line shows the actual infections at a daily frequency. The actual infection ends on September 18, 2022 in the last AB 3-3 report. The subsequent actual data is from the Tokyo Metropolitan Government.

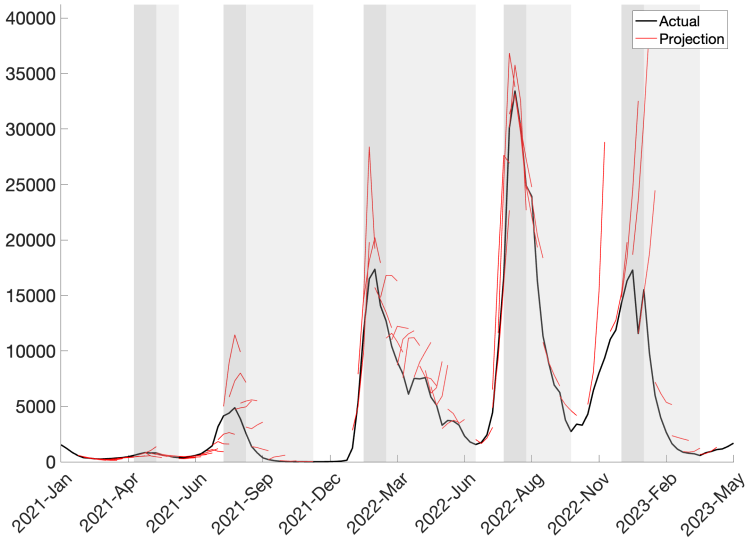

Figure 3: Fujii-Nakata Projection

Note: The solid red lines show four-week-ahead projections of the 7-day moving average of daily new infections at a weekly frequency. Projection data are from their original files. The solid black line shows the actual 7-day moving average of daily new infections at a weekly frequency. The actual data are from the Tokyo Metropolitan Government.

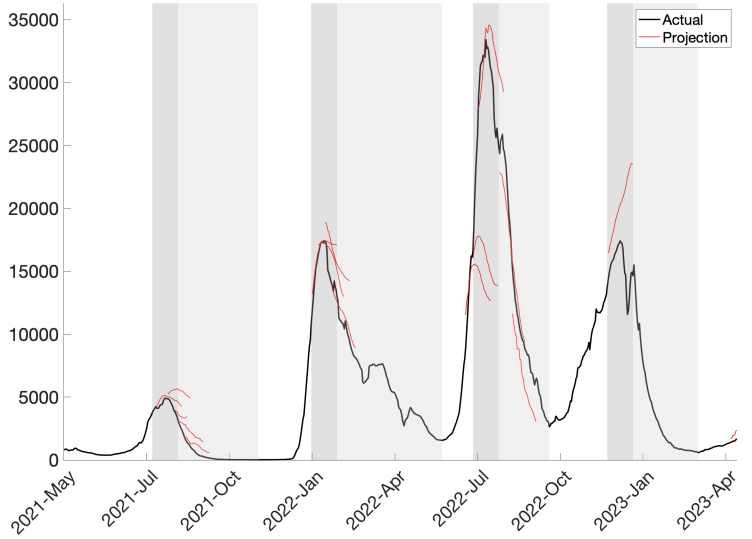

Figure 4: Hirata Projection

Note: The solid red lines show four-week-ahead projections of the 7-day moving average of daily new infections at a daily frequency. Projection data are digitized from the original reports. The solid black line shows the actual 7-day moving average of daily new infections at a daily frequency. The actual data is from the Tokyo Metropolitan Government.

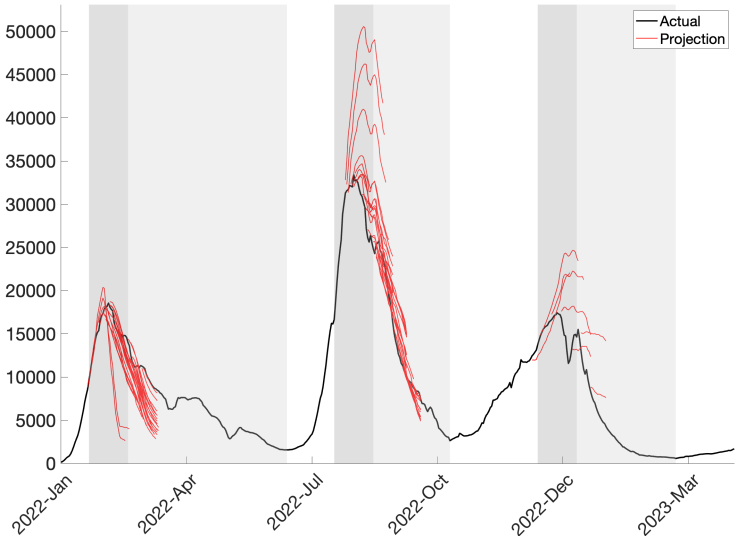

Figure 5: CATs Projection

Note: The solid red lines show four-week-ahead projections of the 7-day moving average of daily new infections at a daily frequency. Projection data is digitized from the original reports. The solid black line shows the actual 7-day moving average of daily new infections at a daily frequency. The actual data is from the Tokyo Metropolitan Government.

Table 1: Projection Accuracy: Entire Samples

Projection horizon	Bias(%)	RMSE(%)	N
AB 3-2			
One week	−3.8	47.7	53
AB 3-3			
One week	−4.6	42.7	74
Two weeks	9.6	87.8	63
Four weeks	166.0**	570.5	63
Fujii-Nakata			
One week	9.0***	27.8	68
Two weeks	20.2***	57.9	68
Four weeks	100.4***	296.8	68
Hirata			
One week	9.0	24.5	16
Two weeks	29.3*	67.5	15
Four weeks	70.6*	146.4	12
CATs			
One week	3.6*	18.3	72
Two weeks	5.0	35.8	63
Four weeks	−18.5*	55.5	26
All projections combined			
One week	1.7	34.7	283
Two weeks	13.1***	64.3	209
Four weeks	104.5***	398.5	169

Note: All projections cover horizons of one, two, and four weeks, except for AB 3-2, which includes only one week. N represents the number of observations. *** $p<0.01$, ** $p<0.05$, * $p<0.10$, based on the two-sided t-test.

Table 2: Projection Accuracy: Wave-by-Wave Analysis

(a) AB 3-2

Projection horizon	Bias(%)	RMSE(%)	N
Sixth wave			
One week	−12.0*	32.3	21
Seventh wave			
One week	19.0	75.8	13
Eighth wave			
One week	−10.3	38.3	16

(b) AB 3-3

Projection horizon	Bias(%)	RMSE(%)	N
Fourth wave			
One week	11.8	36.1	9
Fifth wave			
One week	−9.5	54.1	21
Two weeks	12.0	117.1	19
Four weeks	290.8	849.7	19
Sixth wave			
One week	−4.0	43.2	28
Two weeks	15.0	84.4	28
Four weeks	146.9	484.9	28
Seventh wave			
One week	−1.1	20.8	12
Two weeks	8.1	40.0	12
Four weeks	73.8**	127.4	12
Eighth wave			
One week	−30.3**	33.2	4
Two weeks	−34.9*	41.5	4
Four weeks	−16.0	47.0	4

(c) Fujii-Nakata

Projection horizon	Bias(%)	RMSE(%)	N
Fourth wave			
One week	−4.8	13.3	14
Two weeks	−11.1*	24.2	14
Four weeks	−9.3	33.6	14
Fifth wave			
One week	11.3	35.9	17
Two weeks	46.4*	101.0	17
Four weeks	269.2**	570.7	17
Sixth wave			
One week	16.2*	37.6	15
Two weeks	18.2***	29.0	15
Four weeks	58.1***	74.6	15
Seventh wave			
One week	9.3	19.1	9
Two weeks	17.2	32.4	9
Four weeks	8.4	25.4	9
Eighth wave			
One week	14.1**	18.8	9
Two weeks	33.3**	51.1	9
Four weeks	168.6***	195.5	9

(d) Hirata

Projection horizon	Bias(%)	RMSE(%)	N
Fifth wave			
One week	29.4***	31.0	5
Two weeks	98.8**	111.2	5
Four weeks	251.1	284.7	3
Sixth wave			
One week	4.4	11.7	4
Two weeks	11.2*	13.6	4
Four weeks	28.6*	32.9	4
Seventh wave			
One week	−15.6*	20.7	5
Two weeks	−23.1	33.0	5
Four weeks	−20.5	38.6	4
Eighth wave			
One week	14.7	14.7	1
Two weeks	16.3	16.3	1
Four weeks	60.9	60.9	1

(e) CATs

Projection horizon	Bias(%)	RMSE(%)	N
Sixth wave			
One week	−7.6***	14.0	29
Two weeks	−20.9***	23.4	26
Four weeks	−54.9***	56.2	17
Seventh wave			
One week	8.5***	15.8	36
Two weeks	17.0***	30.7	31
Four weeks	45.3***	48.8	7
Eighth wave			
One week	24.5*	36.9	7
Two weeks	55.2*	78.9	6
Four weeks	68.2	70.3	2

(f) All projections combined

Projection horizon	Bias(%)	RMSE(%)	N
Fourth wave			
One week	1.7	24.8	23
Two weeks	−11.1*	24.2	14
Four weeks	−9.3	33.6	14
Fifth wave			
One week	3.2	45.3	43
Two weeks	36.8**	110.0	41
Four weeks	278.3**	707.1	39
Sixth wave			
One week	−3.3	32.3	97
Two weeks	2.7	55.7	73
Four weeks	65.1	324.2	64
Seventh wave			
One week	7.3*	35.5	75
Two weeks	11.7***	33.4	57
Four weeks	37.4***	83.5	32
Eighth wave			
One week	0.7	33.2	37
Two weeks	25.4**	58.3	20
Four weeks	103.2***	151.3	16

Note: All projections cover horizons of one, two, and four weeks, except for AB 3-2, which includes only one week. N represents the number of observations. *** $p<0.01$, ** $p<0.05$, * $p<0.10$, based on the two-sided t-test. Note that we cannot compute t-statistic when N=1.

Table 3: Projection Accuracy: Phase-by-Phase Analysis

(a) AB 3-2

Projection horizon	Bias(%)	RMSE(%)	N
Rising			
One week	−29.6*	50.5	10
Peak			
One week	8.5	31.0	12
Falling			
One week	0.9	54.5	28

(b) AB 3-3

Projection horizon	Bias(%)	RMSE(%)	N
Rising			
One week	−32.1***	44.1	25
Two weeks	−42.4***	57.1	21
Four weeks	−23.0	124.0	21
Peak			
One week	33.7***	51.0	16
Two weeks	122.7***	166.1	12
Four weeks	861.5**	1289.1	12
Falling			
One week	−2.4	36.9	33
Two weeks	0.8	53.7	30
Four weeks	20.1	89.7	30

(c) Fujii-Nakata

Projection horizon	Bias(%)	RMSE(%)	N
Rising			
One week	6.0	35.1	21
Two weeks	−7.6	30.2	21
Four weeks	−17.4	59.6	21
Peak			
One week	4.9	15.2	21
Two weeks	23.6**	51.2	21
Four weeks	147.6***	266.2	21
Falling			
One week	15.9**	31.2	22
Two weeks	46.6***	83.4	22
Four weeks	189.9**	448.4	22

(d) Hirata

Projection horizon	Bias(%)	RMSE(%)	N
Rising			
One week	−5.5	5.5	1
Two weeks	−40.7	40.7	1
Four weeks	−59.4	59.4	1
Peak			
One week	10.8	24.4	11
Two weeks	34.4*	64.5	11
Four weeks	69.2	139.9	9
Falling			
One week	−4.0	19.3	3
Two weeks	34.1	83.4	3
Four weeks	141.7	196.9	2

(e) CATs

Projection horizon	Bias(%)	RMSE(%)	N
Rising			
One week	−4.8	9.4	2
Two weeks	−2.8	5.0	2
Peak			
One week	4.6*	15.1	40
Two weeks	2.9	27.6	40
Falling			
One week	2.8	22.2	30
Two weeks	9.9	49.0	21

(f) All projections combined

Projection horizon	Bias(%)	RMSE(%)	N
Rising			
One week	−16.7***	41.2	59
Two weeks	−24.4***	44.6	45
Four weeks	−20.1	96.0	45
Peak			
One week	10.5***	27.1	100
Two weeks	29.3***	74.2	84
Four weeks	205.7***	573.0	66
Falling			
One week	3.2	37.7	116
Two weeks	17.9**	63.9	76
Four weeks	93.8**	296.4	54

Note: All projections cover horizons of one, two, and four weeks, except for AB 3-2, which includes only one week. N represents the number of observations. *** $p<0.01$, ** $p<0.05$, * $p<0.10$, based on the two-sided t-test. Note that we cannot compute t-statistic when N=1.

Technical Appendix

A Alternative Definitions of Infection Phases

Table A.1: Peak Phase Defined as a Window of ±7 Days around the Peak

(a) AB 3-2

Projection horizon	Bias(%)	RMSE(%)	N
Rising			
One week	−20.6*	43.4	14
Peak			
One week	2.0	13.7	6
Falling			
One week	3.6	55.6	30

(b) AB 3-3

Projection horizon	Bias(%)	RMSE(%)	N
Rising			
One week	−25.6***	47.7	28
Two weeks	−24.9	89.8	23
Four weeks	127.2	694.4	23
Peak			
One week	36.5***	47.2	9
Two weeks	126.6**	156.1	7
Four weeks	832.0**	1081.0	7
Falling			
One week	1.3	37.3	37
Two weeks	8.9	62.7	33
Four weeks	51.8	193.5	33

(c) Fujii-Nakata

Projection horizon	Bias(%)	RMSE(%)	N
Rising			
One week	6.2	33.0	25
Two weeks	−2.6	35.4	25
Four weeks	−1.2	73.0	25
Peak			
One week	4.9	14.4	13
Two weeks	20.9	47.5	13
Four weeks	138.0**	223.4	13
Falling			
One week	13.8**	29.1	26
Two weeks	44.4***	80.0	26
Four weeks	198.0**	447.4	26

(d) Hirata

Projection horizon	Bias(%)	RMSE(%)	N
Rising			
One week	−2.3	17.9	6
Two weeks	−9.6	27.0	6
Four weeks	13.4	52.0	6
Peak			
One week	13.1	21.8	4
Two weeks	36.6	52.5	4
Four weeks	27.7	33.3	3
Falling			
One week	12.4	27.9	5
Two weeks	70.2	102.8	5
Four weeks	227.8	281.4	3

(e) CATs

Projection horizon	Bias(%)	RMSE(%)	N
Rising			
One week	1.0	8.2	4
Two weeks	−1.5	15.7	4
Peak			
One week	6.3*	17.1	27
Two weeks	6.8	30.0	27
Falling			
One week	2.1	19.7	41
Two weeks	4.3	41.7	32

(f) All projections combined

Projection horizon	Bias(%)	RMSE(%)	N
Rising			
One week	−11.2**	39.4	77
Two weeks	−12.1	61.9	58
Four weeks	51.0	440.6	58
Peak			
One week	10.6***	23.9	59
Two weeks	29.2***	67.9	51
Four weeks	165.8**	449.4	44
Falling			
One week	4.8	36.6	139
Two weeks	20.2***	64.9	96
Four weeks	118.7***	325.7	63

Note: All projections cover horizons of one, two, and four weeks, except for AB 3-2, which includes only one week. N represents the number of observations. *** p<0.01, ** p<0.05, * p<0.10, based on the two-sided t-test.

Table A.2: Peak Phase Defined as a Window of ±10 Days around the Peak

(a) AB 3-2

Projection horizon	Bias(%)	RMSE(%)	N
Rising			
One week	−23.8*	46.7	12
Peak			
One week	11.7	34.5	9
Falling			
One week	0.4	53.6	29

(b) AB 3-3

Projection horizon	Bias(%)	RMSE(%)	N
Rising			
One week	−31.6***	43.4	26
Two weeks	−42.4***	57.1	21
Four weeks	−23.0	124.0	21
Peak			
One week	38.9***	54.8	12
Two weeks	133.7**	178.7	9
Four weeks	1025.8**	1450.9	9
Falling			
One week	0.3	37.3	36
Two weeks	8.9	62.7	33
Four weeks	51.8	193.5	33

(c) Fujii-Nakata

Projection horizon	Bias(%)	RMSE(%)	N
Rising			
One week	6.2	33.0	25
Two weeks	−2.6	35.4	25
Four weeks	−1.2	73.0	25
Peak			
One week	4.9	14.4	13
Two weeks	20.9	47.5	13
Four weeks	138.0**	223.4	13
Falling			
One week	13.8**	29.1	26
Two weeks	44.4***	80.0	26
Four weeks	198.0**	447.4	26

(d) Hirata

Projection horizon	Bias(%)	RMSE(%)	N
Rising			
One week	−6.8	20.8	4
Two weeks	−18.1	32.5	4
Four weeks	−3.2	50.8	4
Peak			
One week	11.0	18.6	6
Two weeks	26.8	43.1	6
Four weeks	35.2**	43.0	5
Falling			
One week	12.4	27.9	5
Two weeks	70.2	102.8	5
Four weeks	227.8	281.4	3

(e) CATs

Projection horizon	Bias(%)	RMSE(%)	N
Rising			
One week	1.0	8.2	4
Two weeks	−1.5	15.7	4
Peak			
One week	5.2*	16.4	33
Two weeks	3.3	27.9	33
Falling			
One week	2.4	20.7	35
Two weeks	8.3	45.7	26

(f) All projections combined

Projection horizon	Bias(%)	RMSE(%)	N
Rising			
One week	−13.7***	38.3	71
Two weeks	−19.2***	44.1	54
Four weeks	−10.1	95.1	54
Peak			
One week	11.9***	28.8	73
Two weeks	28.6***	76.1	61
Four weeks	219.1**	633.5	49
Falling			
One week	4.0	36.5	131
Two weeks	22.4***	67.0	90
Four weeks	121.6***	328.2	62

Note: All projections cover horizons of one, two, and four weeks, except for AB 3-2, which includes only one week. N represents the number of observations. *** $p<0.01$, ** $p<0.05$, * $p<0.10$, based on the two-sided t-test.